 doi:10.20944/preprints202004.0396.v1

Influence of Biocompatible Coating on Titanium Surface Characteristics

Željka Petrović[1,*], Jozefina Katić[2], Ankica Šarić[3], Ines Despotović[4], Nives Matijaković[1], Damir Kralj[1], Mirela Leskovac[5], Marin Petković[6]

[1] Division of Materials Chemistry, Ruđer Bošković Institute, Bijenička cesta 54, 10002 Zagreb, Croatia; zpetrov@irb.hr; Nives.Matijakovic@irb.hr; kralj@irb.hr;
[2] Dept. of Electrochemistry, Faculty of Chemical Engineering and Technology, University of Zagreb, Marulićev trg 19, 10000 Zagreb, Croatia; jkatic@fkit.hr
[3] Division of Materials Physics, Centre of Excellence for Advanced Materials and Sensing Device, Ruđer Bošković Institute, Bijenička cesta 54, 10002 Zagreb, Croatia; Ankica.Saric@irb.hr
[4] Division of Physical Chemistry, Ruđer Bošković Institute, Bijenička cesta 54, 10002 Zagreb, Croatia; Ines.Despotovic@irb.hr
[5] Dept. of Polymer Engineering and Organic Chemical Technology, Faculty of Chemical Engineering and Technology, University of Zagreb, Marulićev trg 19, 10000 Zagreb, Croatia; mlesko@fkit.hr
[6] Adentro dental studio, Petrova ul. 67, 10000 Zagreb, Croatia; info@adentro.hr

*Corresponding author: E-mail:zpetrov@irb.hr; Tel:+385 91 7684985

Abstract:

Background: Nowadays investigations in the field of dental implants engineering are focused on bioactivity and osseointegration properties.

Objective: In this study, the oxide-covered titanium was functionalized by vitamin D3 molecules via a simple self-assembly method with the aim to design more corrosion resistant and at the same time more bioactive surface.

Methods: Surface properties of the D3-coated titanium were examined by scanning electron microscopy, attenuated total reflectance Fourier transform infrared spectroscopy, and contact angle measurements, while a long-term corrosion stability during immersion in an artificial saliva solution was investigated *in situ* by electrochemical impedance spectroscopy.

Results: Results of all techniques confirmed a successful formation of the D3 vitamin layer on the oxide-covered titanium. Besides very good corrosion resistivity (~5 MΩ cm^2) the D3-modified titanium surface induced spontaneous formation of biocompatible bone-like calcium phosphates (CaP).

Conclusion: Observed *in vitro* CaP-forming ability as a result of D3-modified titanium/artificial saliva interactions could serve as a promising predictor of *in vivo* bioactivity of implant materials.

Keywords: titanium; D3 vitamin; self-assembly; surface coating; calcium phosphates; corrosion properties

Preprints (www.preprints.org) | NOT PEER-REVIEWED | Posted: 22 April 2020 doi:10.20944/preprints202004.0396.v1

1. INTRODUCTION

It is well-known that an implantation success depends on the process of osseointegration, which was first described by Swedish professor Brånemark, "father of modern dental implantology" [1,2]. This discovery, that bone can be effectively fixed to the implant without its rejection, launched a new era of investigations and development of dental implant materials [3,4]. From that time until the last decade the research focus shifted from implant's design and geometry to osseoinductive properties of implant surfaces.

Current trends in dental implant research are based on surface properties modifications by biomimetic and bioactive coatings that mimic biochemical surroundings and architecture of the human bone [3-5]. Calcium phosphate ceramics, like hydroxyapatite, with mineral composition similar to natural bone, as a single compound coating or as a composite with collagen, bioglass, or silica are used to promote osseointegration or overall implant system's characteristics [6,7]. Peptide RGD coatings that facilitate cell adhesion during osseointegration are also used to design novel implant surfaces [8]. Drug-based coatings with bisphosphonates like Zolendronate [9] or Alendronate [10,11], drugs for bone diseases, promote mechanical fixation of implant and bone mineralization.

However, it must not be forgotten that a fundamental prerequisite for the success of osseointegration is a long-term corrosion stability of implant materials. Human body fluids, especially oral cavity fluids, in which pH is constantly changing, represent very aggressive media with high concentrations of chloride ions that are among the most aggressive and corrosive to metals [12]. Although, titanium is a gold standard in dental implantology due to its exceptional biocompatibility and corrosion resistivity [12,13], there is an increasing data reported regarding complications caused by titanium dental implant fixation. It was shown that titanium ions, that originated as product from corrosion reaction in body fluids, caused negative immune reactions or skin allergies immediately or shortly after implant fixation [14-16]. Therefore, it is crucial to design a coating which will make titanium surface more bioactive/osseoinductive and at the same time more corrosion resistant during a long-term exposure to oral cavity fluids.

In this study the titanium surface was modified by vitamin D3, molecules that are crucial for normal functioning of the immune system [17] and maintaining bone mineral density [18]. The main goals were (i) to improve titanium corrosion resistivity during exposure to an artificial saliva solution and simultaneously (ii) to induce *in vitro* processes of "new bone" formation. In our previous published paper a D3 coating formation mechanism on the oxide-covered titanium dental implant was explained in detail by DFT method [19] whereas this research is a follow up to previous study and a long-term corrosion behavior of the D3 vitamin-modified titanium surface in an artificial saliva solution was investigated *in situ* by electrochemical impedance spectroscopy. To the best of our knowledge, surface characteristics of bioactive coatings on dental implants are in the focus of current research in this field, but their corrosion stability has not been sufficiently investigated.

2. MATERIALS AND METHODS

2.1. Chemicals, Materials, and Ti Surface Coating Formation

The following chemicals were used as received: Vitamin D3 drops (122 μmol dm^{-3} cholecalciferol in aqueous glycerol solution; ChildLife®, USA), acetone (p.a., Gram-Mol®, Croatia), and absolute ethanol (p.a., Gram-Mol®, Croatia). The titanium discs (Ti, 99.9%, Alfa Aesar®, Karlsruhe, Germany) of 12 mm in diameter were used as substrates for bioactive coating formation.

The Ti surfaces were abraded with SiC emery papers of #240 to #600 grit, ultrasonically cleaned with absolute ethanol and redistilled water, and dried in a stream of nitrogen (99.999%, Messer®, Germany). Prepared Ti discs were electrochemically treated in order to prepare an oxide-covered Ti surface needed for a successful D3 vitamin bonding [19]. The oxide layer on the Ti (Ti/oxide) was formed potentiostatically at the film formation potential, E_f = 2.5 V *vs* Ag|AgCl|3 mol dm^{-3} KCl during 24 hours in a phosphate buffer solution (0.075 mol dm^{-3} $Na_2HPO_4 \cdot 7H_2O$ + 0.025 mol dm^{-3} $NaH_2PO_4 \cdot 2H_2O$, pH 7.4). The Ti/oxide samples were rinsed with redistilled water and dried in a stream of nitrogen. The D3 vitamin layer onto the Ti surface was produced by immersion of the Ti/oxide samples in vitamin D3 solution at 21 ± 1 °C during 24 hours. Thereafter, the modified

Preprints (www.preprints.org) | NOT PEER-REVIEWED | Posted: 22 April 2020 doi:10.20944/preprints202004.0396.v1

samples were dried in a regular air-convection oven (Memmert®, Schwabach, Germany) at 70 °C for 5 hours according to previously reported procedures [19,20]. Ti/oxide/D3 samples were additionally rinsed with absolute ethanol, redistilled water and dried in a stream of nitrogen. Thus prepared Ti/oxide and Ti/oxide/D3 samples were denoted in the text as-prepared samples.

2.2. Characterization Methods

The characterization of samples was performed by contact angle measurements (CA), attenuated total reflectance Fourier transform infrared spectroscopy (ATR-FTIR), thermal field emission scanning electron microscopy (SEM), energy dispersive X-ray analysis (EDS) and electrochemical impedance spectroscopy (EIS).

The contact angle measurements were carried out by a contact angle system OCA 20 (Dataphysics Instruments GmbH, Germany) at 21 ± 2 °C using Milli-Q® water, formamide and diiodomethane at the dosing volume of 1 μl. Values were measured after a 10s-stabilization period at different surface positions. The surface free energy of investigated surfaces was calculated by the software SCA 20 ver. 2.01.

A Tensor II spectrometer (Bruker Optik GmbH, Ettlingen, Germany) was used for ATR-FTIR measurements in the wavenumber range between 4000 and 340 cm^{-1} at 4 cm^{-1} scan step and total 16 scans per measurement.

The samples morphology was examined by a thermal field emission scanning electron microscope (model JSM-7000F, Jeol Ltd., Tokyo, Japan) connected to the Oxford Instruments EDS/INCA 350 energy dispersive X-ray analyzer for elemental analysis.

The corrosion properties of Ti samples in an artificial saliva solution electrolyte, pH 6.8 were explored by EIS at the open circuit potential, E_{OC} during immersion period of 1 hour and 1month. The measurements were performed with an *ac* voltage amplitude of ±5 mV in the frequency range from 10^5 to 10^{-3} Hz by using Solartron 1287 potentiostat/galvanostat with Solartron FRA 1260 (Solartron Analytical, UK) controlled by *ZPlot*® software v. 3.5e. The complex non-linear least squares (CNLS) fit analysis [21] *ZView*® software v. 3.5e was employed to model experimental data with χ^2 values less than 5×10^{-3} (errors in parameter values of 1–5%). The measurements were performed in a standard three-electrode cell (Corrosion Cell K0047, Princeton Applied Research, USA) with a Pt electrode as a counter electrode and a reference electrode, Ag|AgCl|3.0 mol dm^{-3} KCl (E = 0.210 V vs. standard hydrogen electrode, SHE) to which all potentials in the paper are referred. The Ti samples served as a working electrode (an area exposed to the electrolyte, A = 0.98 cm^2). The Fusayama artificial saliva (0.4 g dm^{-3} NaCl, 0.4 g dm^{-3} KCl, 0.6 g dm^{-3} $CaCl_2{\cdot}2H_2O$, 0.58 g dm^{-3} $Na_2HPO_4{\cdot}2H_2O$, and 1 g dm^{-3} urea), pH 6.8 [22], prepared from *p.a*. grade chemicals and redistilled water, was an electrolyte solution.

3. RESULTS AND DISCUSSION

3.1. Morphological and Chemical Properties of Ti Samples

Scanning electron microscopy (SEM) was used to characterize surface features of investigated samples. The morphology of Ti/oxide and Ti/oxide/D3 samples before (as-prepared samples) and after a 1-month immersion period in an artificial saliva solution is presented in Fig. **(1)**. As can be seen, the oxide layer, prepared potentiostatically on the Ti surface, is characterized by a layered-structure and can be divided in two regions: (i) the outer region grown near the oxide layer/phosphate buffer solution interface - inhomogeneous with cracks and (ii) the inner region grown near the Ti/oxide layer interface - more homogeneous and compact. The D3 layer, self-assembled on the Ti/oxide surface, did not change notably the surface morphology due to its low thickness according to our DFT calculations [19]. Besides, it is known that self-assembled films, which are of a monolayer thickness (up to 2 nm), do not influence significantly morphological or other characteristics of the substrate [23].

After a 1-month immersion period of both samples in an artificial saliva solution, the morphology was preserved, but white island features appeared that were also visible by the naked eyes, Figs. **(1cd)**. A deep insight into white islands, Fig. **(2a)** shows 3D architecture composed of flower-like agglomerates (up to 1 mm) self-assembled from needle-shaped nanosized units. Apparently, a process of 3D flower-architecture formation

Preprints (www.preprints.org) | NOT PEER-REVIEWED | Posted: 22 April 2020 doi:10.20944/preprints202004.0396.v1

on both surfaces under experimental conditions (1 month, room temperature, pH = 6.8, and ions present in artificial saliva) was self-induced.

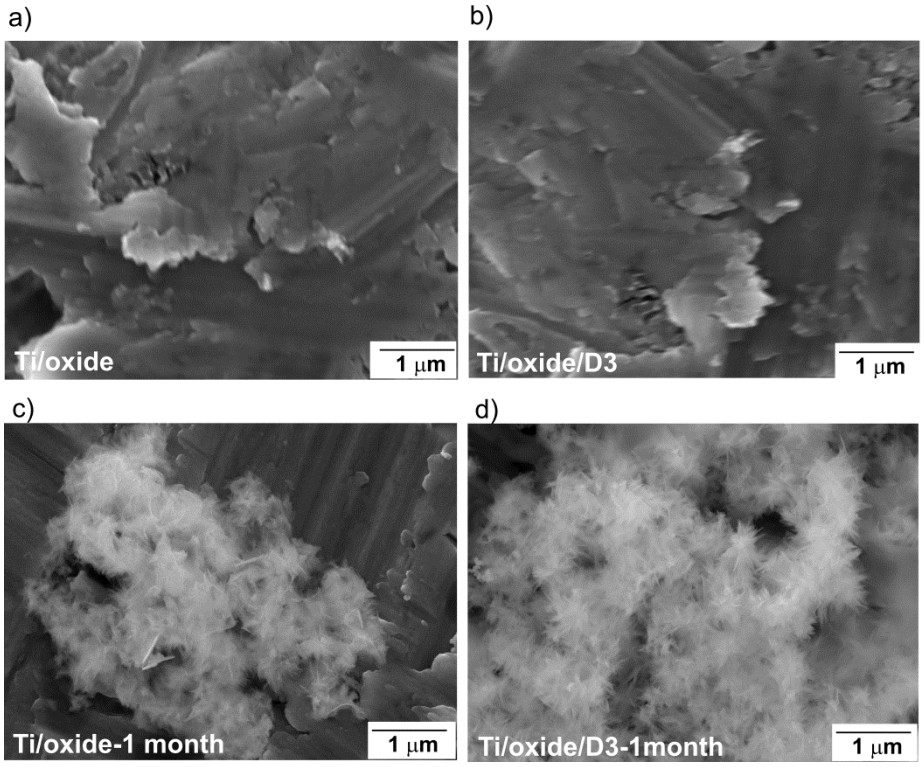

Fig. (1). SEM images of Ti/oxide and Ti/oxide/D3 samples: **(a,b)** before and **(c,d)** after 1 month-immersion period in the artificial saliva solution.

Elemental analysis identified titanium and oxygen on the as-prepared Ti/oxide surface and titanium, oxygen, and carbon on the as-prepared Ti/oxide/D3 surface, Figs. **(1ab)**. On the samples immersed 1 month in the artificial saliva solution Ca, P, Cl, Na, K, O, C, and Ti existed in the region of the white islands features, Figs. **(2ab)**, since in the grey region Ti and O were mainly present. Hence, spontaneously formed 3D-flower architectures are by their chemical composition calcium phosphates, CaP. The CaP is a main component of natural bone tissues along with other trace elements (Na, K, O, F, Mg, and Cl) and it can be found in the form of crystalline hydroxyapatite (HAp) or amorphous calcium phosphate (ACP) [24-26].

According to the elemental analysis, Fig. **(2b**), Ca/P atomic ratio equals to 1.42 and most probably points to an amorphous calcium phosphate, ACP; $Ca_xH_y(PO_4)_z{\cdot}nH_2O$, n = 3-4.5; 15-20% H_2O (Ca/P = 1.2 – 2.2) [24-28]. Due to trace elements detected (Cl, Na, K, O, C), the CaP is biocompatible bone-like CaP that is always nonstoichiometric with structural imperfections co-substituted in the crystal lattice. The presence of trace elements in the CaP formed is advantage due to their important roles in biological processes, especially in bone metabolism and activation of osteoclasts [25]. Larger agglomerates and in a higher amount appeared on the Ti/oxide/D3 surface in comparison to the Ti/oxide surface, as shown in Figs. **(1cd)**. According to the elemental analysis, white islands deposits of very similar composition with the Ca/P = 1.40 were formed on the Ti/oxide surface.

The fabrication and properties of 3D architectures (porous spheres, enamel-like structures, 3D flowers etc.) of biological materials like hydroxyapatite and other CaP forms have attracted great interest due to their enhanced biological performances [25]. Their synthesis is usually carried out in the presence of surfactant, template supporting or structure-directing reagents [25, 28,29], therefore spontaneous CaP formation closely resembling to human bones, makes investigated surfaces osseoinductive. Thus, it can be concluded that the organic D3 vitamin top layer acted as a CaP growth-promotor that stimulated nanoneedles growth as well as their self-assembly in 3D architectures. In addition, it is well known that vitamin D3 is a key factor for the calcium

Preprints (www.preprints.org) | NOT PEER-REVIEWED | Posted: 22 April 2020 doi:10.20944/preprints202004.0396.v1

homeostasis [30] and thus, the titanium surface covered with the D3 vitamin layer is indeed biocompatible since it could attract more calcium and phosphorus than the titanium oxide itself.

Increased *in vitro* CaP-forming ability, as a consequence of biologically active D3 vitamin layer, could serve as a predictor of *in vivo* bioactivity of investigated surfaces.

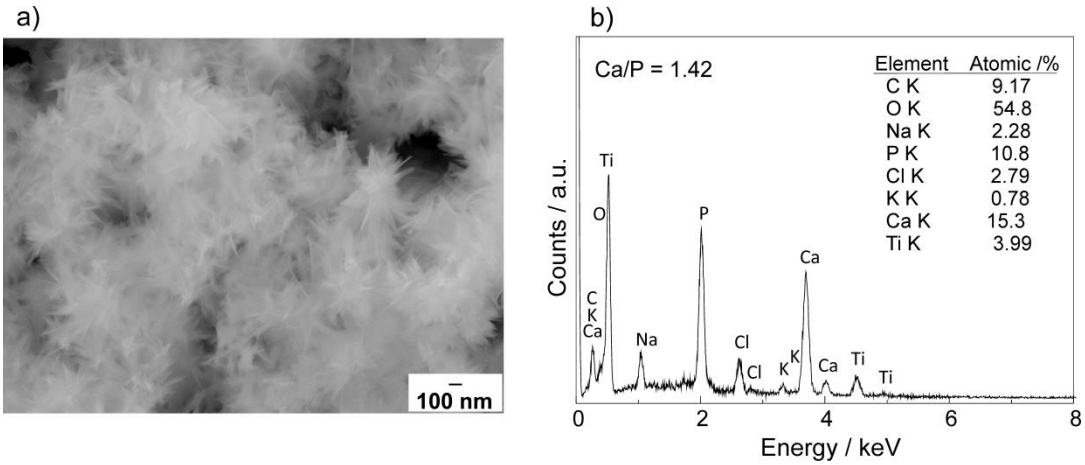

Fig. 2. (a) The morphology of white deposit features spontaneously formed on the Ti/oxide/D3 surface during 1 month-immersion period in the artificial saliva solution and **(b)** corresponding EDS spectrum and chemical composition of the deposit.

The chemistry of Ti/oxide and Ti/oxide/D3 surfaces, before and after 1 month-immersion period, was examined by attenuated total reflection Fourier transform infrared spectroscopy (ATR-FTIR) and corresponding spectra are presented in Fig. **(3)**. The spectra of as-prepared samples, recorded after the final step of modification (see Section 2.1), are shown in Fig. **(3a)**. In the Ti/oxide spectrum, a band at 351 cm^{-1} is related to the Ti-O stretching vibrations [31]. Upon the D3 layer formation on the Ti/oxide surface, a recorded response is more complex than a spectrum of the Ti/oxide sample. Bands characteristic for D3 vitamin can be observed in the spectra and are in accordance with literature data [19, 32]. A presence of a band located at 1643 cm^{-1} that is assigned to the H-C=CH stretching vibration, confirms formation of the D3 vitamin layer on the Ti/oxide surface. Furthermore, the Ti-O band at 351 cm^{-1} is also visible due to relatively low D3 layer thickness [19].

After 1 month-immersion in an artificial saliva solution, ATR-FTIR responses of both samples are different compared to responses of as-prepared samples, Figs. **(3ab)**. The bands assignation was done according to published data [25,26,29,33]. Both samples show a broad band observed in the range from 3700 – 3000 cm^{-1} that corresponds to adsorbed water molecule vibrations. It is also visible a band around 1639 cm^{-1} that can be assigned to water bending mode. In the case of the Ti/oxide/D3 sample this band can be overlapped with band characteristic to H-C=CH stretching vibration of the D3 vitamin, Fig. **(3a)**. The bands at 471 (ν_{2b}), 480 (ν_{2a}), 560 (ν_{4c}), 601 (ν_{4a}), 961 (ν_1), 1025 (ν_{3c}), and 1082 cm^{-1} (ν_{3a}) correspond to PO_4^{3-} vibrations and bands at around 1456 (ν_4/ν_3), 1417 (ν_3) and 861 cm^{-1} (ν_3) indicate a presence of carbonate ions, CO_3^{2-}. A weak band at around 1539 cm^{-1} is assigned to ν(O=C-NH) [34] and originates from urea, component of the artificial saliva in which samples were immersed.

Absorption bands and their locations in ATR-FTIR spectra point to the formation of CaP deposits on both samples, Ti/oxide and Ti/oxide/D3 during their 1 month-immersion in an artificial saliva solution what is in accordance with SEM and EDS results, Figs. **(1,2)**. The appearance of carbonate ions in the CaP structure is quite reasonable, since atmospheric CO_2 could diffuse into the artificial saliva solution during 1 month-immersion period. An additional confirmation of carbonate substitution in the CaP structure is absence of a characteristic OH band at around 3570 cm^{-1} what also can be an indication of non-well-crystallized CaP deposits [25,29]. The carbonate content makes coatings more similar to the natural bone mineral composition [33]. It needs to be pointed out that bands intensities of the Ti/oxide/D3 sample are higher compared to intensities of the Ti/oxide sample what indicates a higher CaP amount on the Ti/oxide/D3 surface and it is in accordance with SEM results.

Preprints (www.preprints.org) | NOT PEER-REVIEWED | Posted: 22 April 2020 doi:10.20944/preprints202004.0396.v1

Based on ATR-FTIR, SEM and EDS results, it could be concluded that the vitamin D3 layer had a strong influence on the spontaneous CaP formation, which means that the surfaces thus prepared exhibited improved bioactivity and osseointegration. In other words, implants whose surface has a greater affinity for spontaneous CaP formation, a material of composition resembling to human bone, will osseointegrate faster with natural bone compared to implants without bioactive surface. These CaP deposits on the D3 vitamin-coated surfaces could act as possible graft materials for a new bone tissue formation.

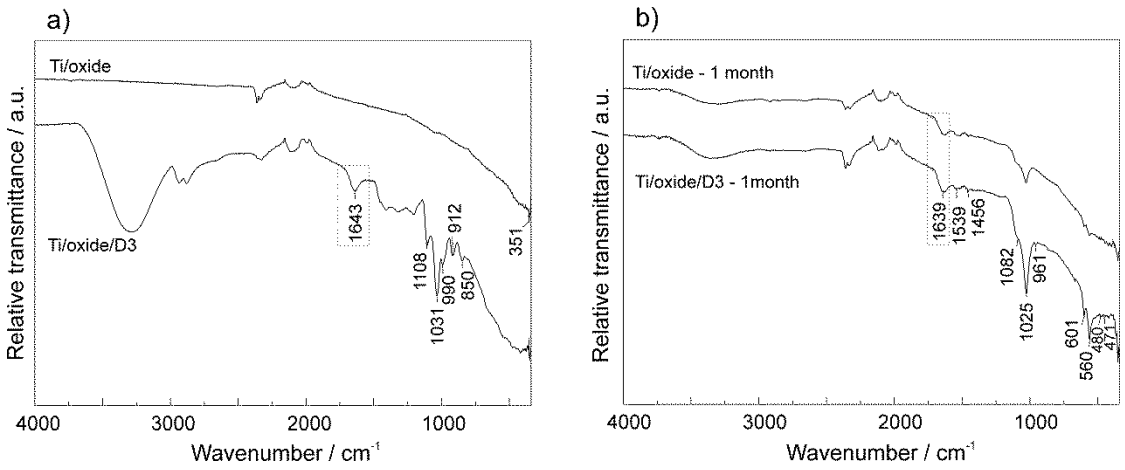

Fig. (3). ATR-FTIR spectra of: **(a)** as-prepared Ti/oxide and Ti/oxide/D3 samples and **(b)** after their 1 month-immersion period in the artificial saliva solution.

3.2. Wetting Properties of Ti Samples

The wetting properties of Ti surfaces before and after 1-month immersion period in an artificial saliva solution were investigated by measuring a static contact angle, θ and results are provided in Table **1**. Wetting properties differences are clearly observed between as-prepared Ti/oxide and Ti/oxide/D3 surfaces. The water contact angle value of the Ti/oxide surface was significantly lower (9.4°) compared to the value measured on the Ti/oxide/D3 surface (42.8°) and pointed to a high hydrophilic character, i.e. an increased wettability of the Ti/oxide surface. Since the oxide film was anodically prepared in a phosphate buffer solution, hydroxyl groups (–OH) present in the outer part of the oxide film, interacted with H_2O drop. Upon a D3 vitamin modification of the Ti/oxide surface, a water contact angle value increased and pointed to more hydrophobic nature of the surface. As confirmed by our previous DFT results [19], D3 molecules are bonded to the oxide surface via Ti-O bond and methyl group ($–CH_3$) as terminal functional group determines the coating's surface properties. Obtained result confirmed a successful D3 layer formation on the Ti/oxide surface.
After 1-month immersion period, contact angle values of both samples were changed due to the precipitation of CaP deposits as was confirmed by SEM, EDS, and ATR-FTIR results, Figs. **(1cd-3)**.

In the field of biomedical applications, solid surface properties and interfacial interactions are of special interest and are determined by the surface free energy. Thus, knowledge of surface free energy values can predict a behavior of implant/bone and implant/surrounding body fluids interactions. Based on contact angle values, the total surface free energy, γ_s and its polar, γ_s^p and dispersive, γ_s^d components of Ti/oxide and Ti/oxide/D3 surfaces were calculated using the Wu's harmonic mean approach, which is an appropriate model for determining the surface free energy of non-polar surfaces like organic liquids and solids [35]:

$$\gamma_{lv}(1+\cos\theta) = \frac{4\gamma_s^d\gamma_l^d}{\gamma_s^d+\gamma_l^d} + \frac{4\gamma_s^p\gamma_l^p}{\gamma_s^p+\gamma_l^p} \quad (1)$$

where θ is the contact angle, γ_{lv} is the interfacial liquid-vapor free energy, γ_l^d, γ_s^d are the dispersive components of the surface free energy of liquid and solid, respectively, and γ_l^p, γ_s^p are the polar components of the surface free energy of liquid and solid, respectively. The surface free energy components of solid (γ_s^p, γ_s^d) for

Preprints (www.preprints.org) | NOT PEER-REVIEWED | Posted: 22 April 2020 doi:10.20944/preprints202004.0396.v1

investigated samples were calculated using numerical values of experimentally determined contact angles and results are given in Table **1**.

According to the total surface free energy value and its components for the as-prepared Ti/oxide sample, polar component of the surface free energy dominates over dispersion component. A polar nature of the anodically formed oxide film is a consequence of –OH groups (present in the outer part of the oxide film) interactions with water molecules via H-bonding. Upon a D3 vitamin modification of the oxide surface, the total surface free energy value decreased compared to the value measured on the Ti/oxide surface due to the presence of a non-polar low-energy component D3 layer, which contains hydrophobic (–CH_2 and –CH_3) groups. Dispersion component of the surface free energy prevails since surface interactions in D3 layer are characterized by van der Waals interactions. It is important to point out that a polar component of the surface free energy is not negligible due to the existence of C-H···O hydrogen bonds in the D3 layer as shown in our DFT study [19].

After 1 month-immersion of the Ti/oxide sample, a decrease of the total surface free energy was induced by significant decrease of the polar component of the surface free energy (Table **1**). Due to spontaneous deposition of the inorganic material, CaP on the oxide surface, H-bonding between –OH groups and water drop were replaced by CaP - water interactions.

The total surface free energy of the Ti/oxide/D3 sample remained nearly unaltered after a prolonged immersion in an artificial saliva solution. Almost equal changes in polar and dispersion component values of the surface free energy before and after spontaneous CaP deposition can be observed in Table **1**. The polar component of the surface free energy increased after 1-month immersion period due to dipole-dipole (adsorbed water - water drop) and/or ion-dipole (phosphate group – water drop and trace elements - water drop) interactions. The presence of water molecules as well as trace elements (ions like Cl^-) is confirmed by ATR-FTIR (Fig. **(3)**) and EDS (Fig. (**2b)**) results. Additionally, the dispersion component of the surface free energy is still present, since irregular CaP islands partially cover the surface and therefore, the water drop can simultaneously sense the D3 coating on the surface as well.

Table 1. Values of contact angles, total surface free energy (γ_s) and its polar (γ_s^p) and dispersive (γ_s^d) components of the Ti samples.

Samples	$\theta(CH_2I_2)$ / °	$\theta(HCONH_2)$ / °	$\theta(H_2O)$ / °	γ_s^p / mJ m^{-2}	γ_s^d / mJ m^{-2}	γ_s/ mJ m^{-2}
As-prepared samples						
Ti/oxide	54.9±1.0	17.5±2.7	9.40±0.4	41.2	25.5	66.7
Ti/oxide/D3	44.4±1.9	41.7±1.3	42.8±1.1	23.9	30.3	54.2
After 1-month immersion in artificial saliva						
Ti/oxide	54.9±1.2	51.1±2.0	56.5±3.0	20.4	28.7	49.1
Ti/oxide/D3	66.2±2.2	54.2±2.2	36.0±1.9	34.7	22.4	57.1

3.3. Corrosion Properties of Ti Samples in Artificial Saliva Solution

The corrosion properties of titanium, Ti/oxide, and Ti/oxide/D3 samples were examined by electrochemical impedance spectroscopy (EIS), a reliable non-destructive technique for *in situ* examination of the corrosion behavior of (un)coated metallic materials. Investigations were performed in an artificial saliva solution electrolyte, pH 6.8, at the open circuit potential, E_{OC} over the wide frequency range after electrolyte-exposure period of 1 hour and 1 month and the results are presented in Fig. **(4)**. For comparison to modified Ti samples, EIS results of the unmodified Ti sample (Ti) is also presented.

Preprints (www.preprints.org) | NOT PEER-REVIEWED | Posted: 22 April 2020 doi:10.20944/preprints202004.0396.v1

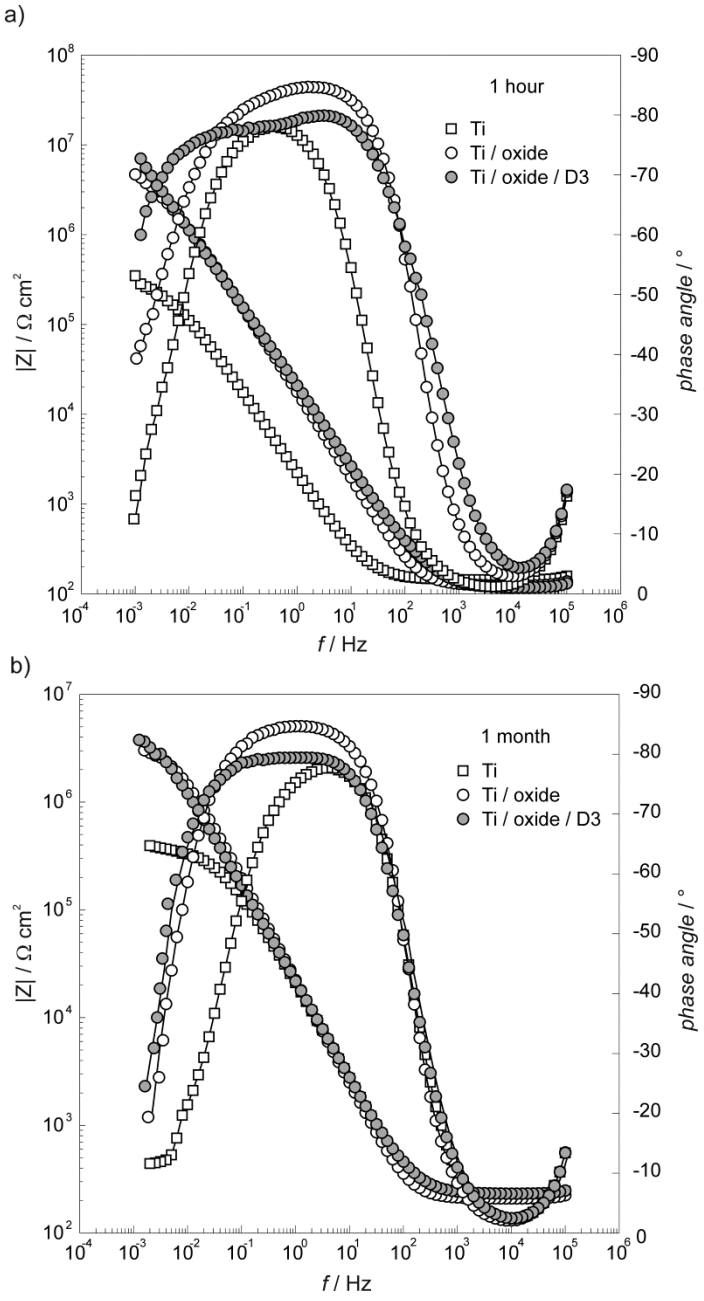

Fig. (4). The Bode plots of Ti, Ti/oxide, and Ti/oxide/D3 samples recorded at E_{OC} in the artificial saliva solution, pH 6.8 after immersion period of **(a)** 1 hour and **(b)** 1 month. Symbols—the experimental data; solid lines—the modeled data.

The EIS data obtained were modeled to the electric equivalent circuit (EEC) consisting of two time constants in a parallel combination connected in series with ohmic (electrolyte) resistance, R_{el} – EEC schematically given as $R_{el}(CPE_1(R_1(CPE_2R_2)))$. The constant phase element (CPE) was utilized instead of capacitor in order to take into account various system's non-homogeneous behavior occurrences (e.g., electrode surface heterogeneity, inhomogeneous current flow, capacitance dispersion) [36,37]. The CPE is characterized by CPE frequency-independent constant, Q and CPE power n as impedance parameters correlated in empirical impedance function $Z_{CPE}=[Q(j\omega)^n]^{-1}$ where ω is the angular frequency. [36] The ideal capacitor is described by n=1, whilst upon surface heterogeneity, the existence of surface films or continuously distributed time constants for charge-transfer reactions $n\neq1$ [36]. For n values higher than 0.8, the interface capacitance values were assessed employing Brug's equation: [37]

Preprints (www.preprints.org) | NOT PEER-REVIEWED | Posted: 22 April 2020 doi:10.20944/preprints202004.0396.v1

$$C = Q^{1/n} [R_{el}^{-1} + R^{-1}]^{(n-1)/n} \quad (2)$$

The impedance parameter values obtained by described EEC model utilization are given in Table **2**.

For the Ti sample (Ti) and Ti sample coated by potentiostatically formed oxide film (Ti/oxide) provided impedance parameters can be correlated to the bi-layered oxide film structure formed on the titanium as a typical model for surface oxide films formed on valve metals including titanium [19, 38-40]. It is known that the titanium surface is always covered by a very thin, spontaneously formed protective passive film. Therefore, the first time constant (CPE_1-R_1), high/middle frequency region, is attributed to the outer part of the oxide layer spontaneously or potentiostatically formed on the Ti surface with R_1 as the resistance and Q_1 as the interfacial capacitance of the oxide outer part. The second time constant (CPE_2-R_2), low frequency region, is ascribed to the inner part of the oxide layer mostly composed of titanium (IV) oxide [12,41] with CPE_2 and R_2 corresponding to the capacitance and the resistance of the oxide inner layer. As can be seen from Table **2**, structural sensitive parameter, CPE power n indicates a porous nature of the outer part (n_1) and more compact inner part (n_2) of both samples. However, the potentiostatically formed oxide film exhibits higher R_2 value attributed to the formation of more compact and corrosion resistant oxide film.

On the other hand, for the (Ti/oxide/D3) sample the two time constants are related to the outer and inner part of the surface coating – vitamin D3 layer over the oxide layer formed. The phase angle as structural sensitive value reflects changes inside the interfacial layer upon (Ti/oxide) surface functionalization by the vitamin D3 layer, Fig. **(4a)**. Induced changes are also reflected in CPE power n_1 value that significantly increased compared to n_1 values of Ti and Ti/oxide samples (Table **2**). The result indicates that vitamin D3 molecules covered / filled in imperfections of the oxide film and the resulting coating (oxide + D3 layer) acted as an effective barrier between the electrolyte and the underlying titanium as can be noticed from significantly increased R_2 values (in order of 10^7 **Ω** cm^2). Since overall corrosion resistance of investigated samples in an artificial saliva solution is defined by the sum of both R_1 and R_2 resistance values equal to the corrosion (polarization) resistance, R_p [42], the subsequent formation of vitamin D3 layer over the oxide layer significantly improved overall corrosion resistance of the underlying Ti sample.

In order to predict a long-term electrochemical/chemical stability of dental implant materials in an aggressive medium such as oral cavity fluids, a corrosion behavior of investigated samples in an artificial saliva solution after 1-month immersion period was examined by EIS and results are presented in Fig. **(4b)** and Table **2**. As can be seen from Table **2**, the prolonged immersion period affected the outer part of the surface films what is reflected in the R_1 values. In more detail, the Ti sample, covered by the spontaneously formed oxide film, exhibited alike impedance parameters during 1 month immersion period, whilst Ti/oxide and Ti/oxide/D3 samples exhibited higher R_1 values related to spontaneous formation of calcium phosphate (CaP) agglomerates on the modified Ti surfaces compared to the Ti sample. The spontaneous CaP formation is corroborated by SEM/EDS, ATR-FTIR, and contact angle measurement results, Figs. **(1-3)**.

The overall corrosion resistance of the Ti/oxide and Ti/oxide/D3 samples, determined by both resistance contributions, decreased during exposure to an artificial saliva solution, which is particularly reflected in R2 values. As it is evident from Figs. (4ab) (phase angle >-90°) and CPE power n values, n < 1, all investigated samples do not behave as ionic insulator due to microstructural imperfections in the coatings' structure, which most likely originate from coating formation procedure. These imperfections allowed ion/water penetration through the coating to the underlying titanium. Since the artificial saliva solution represents an aggressive medium, a high amount of chloride ions affects the surface film properties and accelerates the titanium corrosion process during a prolonged immersion period [19,40]. The spontaneously formed fluffy 3D CaP clusters, which partially cover Ti/oxide and Ti/oxide/D3 surfaces, do not provide additional corrosion protection to the titanium, but make its surface osseoinductive what is of great importance in dental implantology application.

The corrosion protection effectiveness, η, of the coated Ti surface can be calculated using the relation: $\eta = (R_{p(modified)} - R_{p(unmodified)})/ R_{p(modified)})$ where $R_{p(unmodified)}$ and $R_{p(modified)}$ are the polarization resistances of unmodified (Ti) and modified Ti (Ti/oxide and Ti/oxide/D3) samples. Despite the decreased resistance values, the overall corrosion resistance (protection effectiveness) after 1 month immersion is 92.0 % and 95.1 % for Ti/oxide and Ti/oxide/D3 interfaces, respectively. Thus, surface films formed impart good corrosion protection level to the underlying Ti material.

In conclusion, titanium material's surface functionalization by vitamin D3 coating resulted in improved corrosion resistance in aggressive cavity fluids (artificial saliva solution), under real dental implant application

conditions. At the same time, the spontaneously induced formation of bone-like calcium phosphates on the D3 vitamin modified Ti surface during a prolonged exposure to artificial saliva solution, confirmed enhanced titanium's bioactivity level.

Table 2. Impedance parameters calculated for EIS data of Ti samples recorded at E_{OC} in the artificial saliva solution, pH 6.8 after different immersion period denoted.

	R_{el} / Ω cm^2	$10^6 \times Q_1$ / Ω^{-1} cm^{-2} s^n	n_1	R_1 / Ω cm^2	C_1 / μF cm^{-2}	$10^6 \times Q_2$ / Ω^{-1} cm^{-2} s^n	n_2	R_2 / MΩ cm^2	C_2 / μF cm^{-2}
*Immersion period of **1 hour***									
Ti	115	6.14	0.648	31.8	/	80.5	0.905	0.27	49.2
Ti/oxide	91	2.03	0.697	37.1	/	8.31	0.974	6.08	6.86
Ti/oxide/D3	117	3.69	0.970	312	2.88	6.02	0.825	23.3	1.29
*Immersion period of **1 month***									
Ti	168	3.01	0.635	69.7	/	6.88	0.933	0.39	4.24
Ti/oxide	210	5.95	0.982	370	5.22	2.00	0.815	3.39	0.34
Ti/oxide/D3	231	4.87	0.955	522	3.48	4.12	0.811	5.56	0.81

CONCLUSION

The titanium surface was modified by the potentiostatically formed oxide and the vitamin D3 coating over the oxide. The influence of prepared coatings on titanium surface characteristics was examined by SEM/EDS, ATR-FTIR, contact angle, and EIS measurements. Results of all techniques confirmed a successful formation of both coatings on the titanium surface.

The long-term electrochemical/chemical stability of coated titanium samples during exposure to the artificial saliva solution was investigated *in situ* by using EIS and results were modeled employing electrical equivalent circuit. Results point to decreased overall corrosion resistivity of the Ti/oxide/D3 as well as Ti/oxide samples after 1-month immersion period compared to values measured after 1-hour immersion period. Ion/water penetration into coatings' structure to the underlying titanium was enabled through structural imperfections what caused the titanium corrosion process. However, surface coatings imparted good corrosion protection level to the titanium, since overall protection effectiveness, after 1-month immersion, amounts 95.1 % and 92.0 % for Ti/oxide/D3 and Ti/oxide, respectively.

The spontaneous formation of biocompatible bone-like calcium phosphates (CaP) during a prolonged immersion in the artificial saliva solution was observed on Ti/oxide/D3 and Ti/oxide surfaces by SEM/EDS, ATR-FTIR, and contact angle measurements. ATR-FTIR and SEM results point out a higher CaP amount on the Ti/oxide/D3 surface compared to amount on the Ti/oxide surface.

The results presented could be useful for designing dental implant surfaces of good anticorrosion properties and at the same time of improved bioactivity. Formed CaP layer can impact interplay of osseointegration and bone growth and in turn resulting in successful implantation and longer life-time of implants.

CONSENT FOR PUBLICATION

Not applicable.

FUNDING

This research received no external funding.

CONFLICT OF INTEREST

The authors declare no conflict of interest.

ACKNOWLEDGEMENTS

This work has been partially supported by SAFU, project KK.01.1.1.01.0001.

REFERENCES

[1] Brånemark PI, Adell R, Breine U, Hansson BO, Lindström J, Ohlsson A. Intra-osseous anchorage of dental prostheses. I. Experimental studies. Scand J Plast Reconstr Surg 1969; 3: 81–100.
[2] Brånemark PI, Adell R, Albrektsson T, Lekholm U, Lundkvist S, Rockler B. Osseointegrated titanium fixtures in the treatment of edentulousness. Biomaterials 1983; 4: 25–28.
[3] Gaviria L, Salcido JP, Guda T, Ong JL. Current trends in dental implants. J Korean Assoc Oral Maxillofac Surg 2014; 40: 50–60.
[4] Smeets R, Stadlinger B, Schwarz F, *et al.* Impact of Dental Implant Surface Modifications on Osseointegration. Biomed Res Int 2016; 2016: 6285620.
[5] Al Mugeiren OM, Baseer MA. Dental Implant Bioactive Surface Modifiers: An Update. J Int Soc Prev Community Dent 2019; 9: 1–4.
[6] Choi AH, Ben-Nissan B, Matinlinna JP, Conway RS. Current Perspectives: Calcium Phosphate Nanocoatings and Nanocomposite Coatings in Dentistry. J Dent Res 2013; 92: 853-859.
[7] Hägi TT, Enggist L, Michel D, Ferguson SJ, Liu Y, Hunziker EB. Mechanical insertion properties of calcium-phosphate implant coatings. Clin Oral Implants Res 2010; 21: 1214–1222.
[8] von Wilmowsky C, Moest T, Nkenke E, Stelzle F, Schlegel KA. Implants in bone: Part I. A current overview about tissue response, surface modifications and future perspectives. Oral Maxillofac Surg 2014; 18: 243–257.
[9] Peter B, Pioletti DP, Laib S, *et al.* Calcium phosphate drug delivery system: influence of local zoledronate release on bone implant osteointegration. Bone 2005; 36: 52–60.
[10] Abtahi J, Tengvall P, Aspenberg P. A bisphosphonate-coating improves the fixation of metal implants in human bone. A randomized trial of dental implants. Bone 2012; 50: 1148–1151.
[11] Rojo L, Gharibi B, McLister R, Meenan BJ, Deb S. Self-assembled monolayers of alendronate on Ti6Al4V alloy surfaces enhance osteogenesis in mesenchymal stem cells. Sci Rep 2016; 6: 30548.
[12] Hansen DC. Metal Corrosion in the Human Body: The Ultimate Bio-Corrosion Scenario. Electrochem Soc Interface 2008: 4.
[13] Eliaz N. Corrosion of Metallic Biomaterials: A Review. Materials 2019; 12: 407-498.
[14] Sicilia A, Cuesta S, Coma G, *et al.* Titanium allergy in dental implant patients: a clinical study on 1500 consecutive patients. Clin Oral Implants Res 2008; 19: 823–835.
[15] Syed M, Chopra R, Sachdev V. Allergic Reactions to Dental Materials-A Systematic Review. J Clin Diagn Res 2015; 9: ZE04-09.
[16] Yan H, Afroz S, Dalanon J, Goto N, Hosoki M, Matsuka Y. Metal allergy patient treated by titanium implant denture: A case report with at least 4-year follow-up. Clin Case Rep 2018; 6: 1972–1977.
[17] Trybek G, Aniko-Włodarczyk M, Kwiatek J, *et al.* The effect of vitamin D3 on the osteointegration of dental implants article details. Balt J Health Phys Act 2018; 10: 25-33.
[18] Atkins GJ, Anderson PH, Findlay DM, *et al.* Metabolism of vitamin D3 in human osteoblasts: Evidence for autocrine and paracrine activities of 1α,25-dihydroxyvitamin D3. Bone 2007; 40: 1517–1528.
[19] Katić J, Šarić A, Despotović I, Matijaković N, Petković M, Petrović Ž. Bioactive Coating on Titanium Dental Implants for Improved Anticorrosion Protection: A Combined Experimental and Theoretical Study. Coatings 2019; 9: 612.
[20] Quiñones R, Gawalt ES. Study of the Formation of Self-Assembled Monolayers on Nitinol Langmuir 2007; 23: 10123–10130.
[21] Boukamp A. A Nonlinear Least Squares Fit procedure for analysis of immittance data of electrochemical systems. Solid State Ionics 1986; 20: 31-44.
[22] Mellado-Valero A, Muñoz AI, Pina VG, Sola-Ruiz MF. Electrochemical Behaviour and Galvanic Effects of Titanium Implants Coupled to Metallic Suprastructures in Artificial Saliva. Materials 2018; 11: 171-190.
[23] Zamborini FP, Crooks RM. Corrosion Passivation of Gold by n-Alkanethiol Self-Assembled Monolayers: Effect of Chain Length and End Group. Langmuir 1998; 14: 3279-3286.

[24] Heimann RB, Lehmann HD. Bioceramics Coatings for Medical Implants: Trends and Techniques. 1st ed. Wiley-VCH; 2015. 69 p.
[25] Lin K, Zhou Y, Zhou Y, *et al.* Biomimetic hydroxyapatite porous microspheres with co-substituted essential trace elements: Surfactant-free hydrothermal synthesis, enhanced degradation and drug release. J Mater Chem 2011; 21: 16558–16565.
[26] Berzina-Cimdina L, Borodajenko N. Research of Calcium Phosphates Using Fourier Transform Infrared Spectroscopy. In: Teophile T, ed. Infrared Spectroscopy - Materials Science, Engineering and Technology [Internet]. Rijeka: IntechOpen; 2012 [cited 2019 Nov 3]. Chapter 6. Available from: DOI: 10.5772/36942
[27] Buljan Meić I, Kontrec J, Domazet Jurašin D, *et al.* Comparative Study of Calcium Carbonates and Calcium Phosphates Precipitation in Model Systems Mimicking the Inorganic Environment for Biomineralization. Cryst Growth Des 2017; 17;1103–1117.
[28] Lin K, Wu C, Chang J. Advances in synthesis of calcium phosphate crystals with controlled size and shape. Acta Biomater 2014; 10: 4071–4102.
[29] Zalite V, Locs J. Characterization of Different Hydroxyapatite Particles for Tooth Enamel Remineralization. Key Eng Mater 2016; 674: 139-144.
[30] Veldurthy V, Wei R, Oz R, Dhawan P, Jeon YH, Christakos S. Vitamin D, calcium homeostasis and aging. Bone Res 2016; 4: 16041.
[31] Ferreira CC, Ricci VP, de Sousa LL, Mariano NA, Campos MGN. Improvement of Titanium Corrosion Resistance by Coating with Poly-Caprolactone and Poly-Caprolactone/Titanium Dioxide: Potential Application in Heart Valves. Mater Res 2017; 20: 126–133.
[32] Othayoth R, Mathi P, Bheemanapally K, Kakarla L, Botlagunta M. Characterization of vitamin-cisplatin-loaded chitosan nano-particles for chemoprevention and cancer fatigue. J Microencapsul 2015; 32,: 578–588.
[33] Dorozhkin SV. Amorphous calcium (ortho)phosphates. Acta Biomater 2010; 6: 4457–4475.
[34] Fischer PHH. Mcdowell CA. The Infrared Absorption Spectra Of Urea–Hydrocarbon Adducts. Can J Chem 1960; 38: 187-193.
[35] Wu S. Polar and Nonpolar Interactions in Adhesion. J Adhes 1973; 5: 39–55.
[36] Orazem ME, Tribollet B. Electrochemical Impedance Spectroscopy. 2nd ed. New York: John Wiley & Sons, 2008. 233 p.
[37] Brug GJ, van den Eeden ALG, Sluyters-Rehbach M, Sluyters JH. The analysis of electrode impedances complicated by the presence of a constant phase element. J Electroanal Chem 1984; 176: 275–295.
[38] Pan J, Thierry D, Leygraf C. Electrochemical impedance spectroscopy study of the passive oxide film on titanium for implant application. Electrochim Acta 1996; 41: 1143–1153.
[39] Aziz-Kerrzo M, Conroy KG, Fenelon AM, Farrell ST, Breslin CB. Electrochemical studies on the stability and corrosion resistance of titanium-based implant materials. Biomaterials 2001; 22: 1531–1539.
[40] Tamilselvi S, Murugaraj R, Rajendran N. Electrochemical impedance spectroscopic studies of titanium and its alloys in saline medium. Mater Corros 2007; 58: 113–120.
[41] Kosec T, Legat A, Kovač J, Klobčar D. Influence of Laser Colour Marking on the Corrosion Properties of Low Alloyed Ti. Coatings 2019; 9: 375.
[42] Scully JR. Polarization Resistance Method for Determination of Instantaneous Corrosion Rates. Corrosion 2000; 56: 199–218.